

High Pressure Research on Materials

1. Production and Measurement of High Pressures in the Laboratory

P Ch Sahu and N V Chandra Shekar



P Ch Sahu (left) is at the Materials Science Division of Indira Gandhi Centre for Atomic Research, Kalpakkam. He is a specialist in the field of high pressure science and is presently heading this activity at his institute.

N V Chandra Shekar (right) is a Senior Scientist at the Materials Science Division of Indira Gandhi Centre for Atomic Research, Kalpakkam. His primary research areas are in high pressure phase transitions and in synthesis and study of novel materials under extreme pressure and temperature conditions.

In this article, different methods for generating and measuring high pressure are described. Empirical equations of state (EOS) are illustrated for some standard materials.

1. Introduction

Pressure, like temperature is an important thermodynamic parameter in our daily life. We use pressure cookers in our kitchen to cook food and use gas cylinders containing LPG at high pressures as fuel. We fill air at high pressures in our bicycle tubes. The pressure inside the earth increases as we go deeper and at the centre, it is estimated to be 360 GPa. It is indeed interesting and challenging to understand the state of matter at such extreme pressures in the interiors of stars and planets. In this article, starting with the definition of pressure and its units, various methods for generating and measuring static high pressures are presented. A brief introduction on dynamic high pressures is also included.

2. Definition of Hydrostatic Pressure

Pressure is defined as force per unit area. However, when we apply force on a body, we generate *stress* (also defined as force per unit area). Under certain special conditions, we call the stress as ‘hydrostatic pressure’. Consider the stress state at point O represented by an *infinitesimal* cube (*Figure 1*). Here σ_{xy} , for example, represents the stress on the x plane in the y direction. There are three stress components on each of its six faces: one direct or normal stress and two shear stresses. The nine stress components from three planes needed to describe the stress state

Key words

Hydrostatic pressure, stress, opposed anvils, diamond anvil cell, hughoniot.



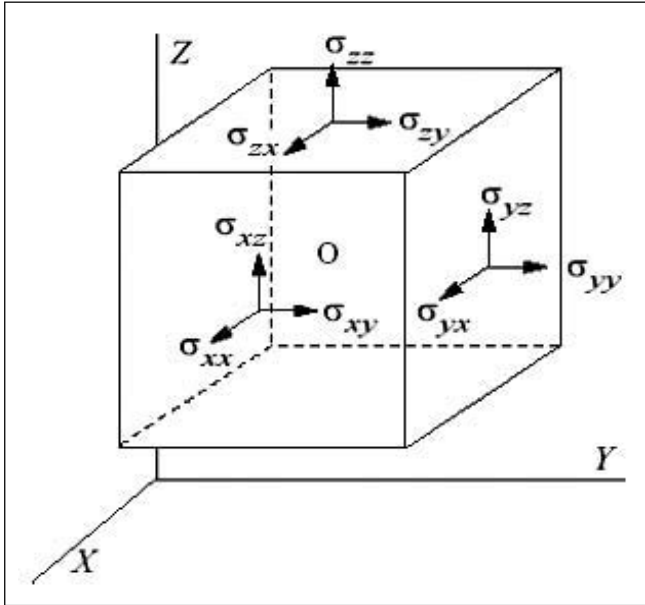


Figure 1. Infinitesimal material cube showing the nine components of the stress tensor.

at the point O can be organized into the matrix:

$$\mathbf{S} = \begin{bmatrix} \sigma_{xx} & \sigma_{xy} & \sigma_{xz} \\ \sigma_{yx} & \sigma_{yy} & \sigma_{yz} \\ \sigma_{zx} & \sigma_{zy} & \sigma_{zz} \end{bmatrix} \quad (1)$$

The off-diagonal shear stresses are equal (i.e. $\sigma_{xy} = \sigma_{yx}$, $\sigma_{xz} = \sigma_{zx}$ and $\sigma_{yz} = \sigma_{zy}$) as a result of static equilibrium. This grouping of nine stress components represents the *stress tensor*.

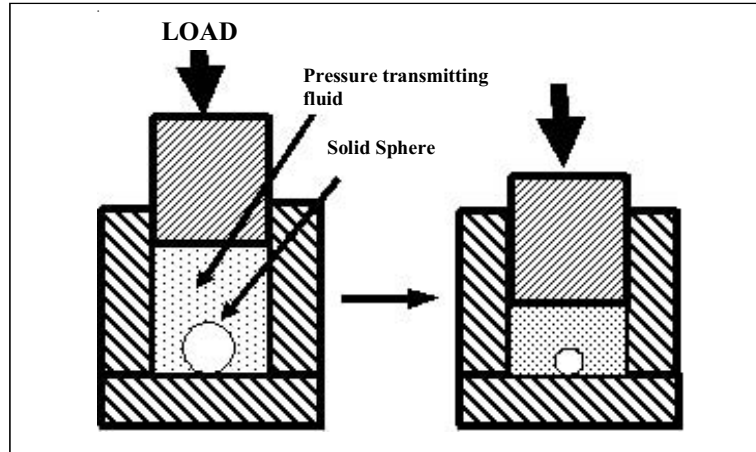
It is convenient to resolve the stress tensor \mathbf{S} into the hydrostatic part \mathbf{S}' and the deviatoric part \mathbf{S}'' , such that $\mathbf{S} = \mathbf{S}' + \mathbf{S}''$:

$$\mathbf{S}' = \begin{bmatrix} \sigma_m & 0 & 0 \\ 0 & \sigma_m & 0 \\ 0 & 0 & \sigma_m \end{bmatrix} \quad (2)$$

$$\mathbf{S}'' = \begin{bmatrix} \sigma_{xx} - \sigma_m & \sigma_{xy} & \sigma_{xz} \\ \sigma_{yx} & \sigma_{yy} - \sigma_m & \sigma_{yz} \\ \sigma_{zx} & \sigma_{zy} & \sigma_{zz} - \sigma_m \end{bmatrix} \quad (3)$$



Figure 2. Shape of a spherical object after subjecting it to hydrostatic pressure.



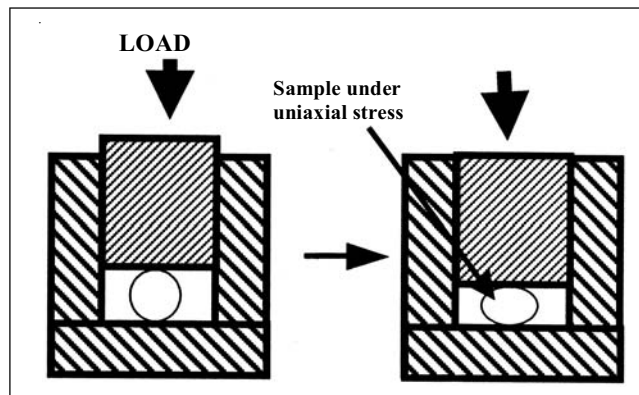
Here, $\sigma_m = (\sigma_{xx} + \sigma_{yy} + \sigma_{zz})/3$. The state of stress S is called hydrostatic if $S'' = 0$, which happens when $\sigma_m = \sigma_{xx} = \sigma_{yy} = \sigma_{zz}$ and $\sigma_{ij} (i \neq j) = 0$.

In practice, hydrostatic stress is achieved by immersing the body in a pressurized fluid medium (as shown in *Figure 2*). The fluid medium also ensures that the load is transmitted slowly. *Figure 2* shows the shape of a spherical object after subjecting it to hydrostatic stress, and *Figure 3* shows the effect of a uniaxial stress.

3. Generation of High Pressure

For generation of high pressures, P W Bridgman (see *Box 1*), introduced most of the fundamental concepts, built and tested the

Figure 3. Shape of a spherical object after subjecting it to uniaxial stress.



Box 1. Percy Williams Bridgman (1882–1961)

P W Bridgman, considered the father of ‘Modern High Pressure Research’, was born in Cambridge, Massachusetts, USA in 1882.. He began his experimental work on the static pressure in 1906 while doing his Phd at Harvard University. By inventing much of the experimental equipment himself, Bridgman extended the pressures achievable in the laboratory to 400,000 atmospheres. His important invention of self sealing gasket, made his work at very high pressures possible. His studies basically involved the measurement of compressibilities of liquids and solids and the phase changes of solids under pressure. His experimentation led to eventual synthesis of diamonds by scientists of the General Electric Company in 1955. He became full Professor at Harvard in 1919. He was awarded Nobel Prize in Physics in 1946 for his work in the domain of high pressure physics. Bridgman published more than 260 papers (only two of which listed a coauthor) and 13 books. His scientific papers have been published in *Collected Experimental Papers* in 7 volumes. Among his many books are *The Physics of High Pressure* (1931) and *Reflections of a Physicist* (1950). In 1961, Bridgman took his own life after he was afflicted with cancer.



Source: www.brittanica.com

basic types of apparatus that are now being used throughout the world. He was awarded the Nobel Prize in Physics in 1946. The static high pressure generating devices can be divided into two categories: piston-cylinder and opposed anvil devices. These devices with their pressure capabilities are listed in *Figure 4*. Different pressure units are described in *Box 2*.

Box 2. Units of Pressure

One atmospheric pressure is defined as the force exerted on a unit surface at sea level by the weight of the air above that surface. It is equal to the pressure exerted by 760 mm column of Hg. The SI unit of pressure Pascal (Pa), defined as $1 \text{ Pa} = 1 \text{ N/m}^2$, is a very small unit compared to 1 atmosphere. There is another practical unit of pressure called bar and $1 \text{ bar} = 10^5 \text{ Pa} = 10^6 \text{ dynes/cm}^2$ (1 atmosphere = 1.01325 bar). In high pressure literature, MPa (10^6 Pa) and GPa (10^9 Pa) are generally used. The most commonly used unit is kilobar or kbar (1000 bar). Some easy to remember conversion relations are: $1 \text{ MPa} = 10 \text{ bar}$, $1 \text{ GPa} = 10 \text{ kbar}$ and $1 \text{ TPa (tera-Pascal)} = 10 \text{ mbar (mega-bar)}$.



TYPE	SCHEMATIC	MATERIALS	PRESSURE RANGE
PISTON/ CYLINDER		PISTON:TUNGSTEN CARBIDE BODY:TEMPERED HIGH STRENGTH STEEL	~ 3GPa
SUPPORTED PISTON/ CYLINDER		PISTON:TUNGSTEN CARBIDE BODY:TEMPERED HIGH STRENGTH STEEL	~ 8GPa
OPPOSED BRIDGMAN ANVILS		TUNGSTEN CARBIDE	~ 15GPa
SUPPORTED ANVILS		TUNGSTEN CARBIDE	~ 25GPa
ANVIL AND SUPPORTED GIRDLE		TUNGSTEN CARBIDE	~ 8GPa
MULTIPLE ANVILS		TUNGSTEN CARBIDE	~ 8GPa
DAC		DIAMOND	>500GPa

 PRIMARY FORCE
 SUPPORTING STRESSES

Figure 4. Schematic representation of principal methods of high pressure generation and their pressure capabilities.

The opposed anvil device works on the ‘Principle of Massive Support’. The principle is a laboratory analogue of the tapered foundation design, to support the large loads of huge structures by the comparatively softer earth. The taper reduces the large working stresses quickly to tolerable levels. The basic design of the anvils (called Bridgman anvils) is shown in *Figure 5*. By applying high enough load on the larger area (loading face) of the anvils, a large stress is generated at the smaller area (working face). A non-metallic gasket is used to house the sample and the pressure transmitter, and to convert the stress into hydrostatic pressure in the sample region. Generally, pyrophyllite (hydrous aluminium silicate – $\text{Al}_4\text{Si}_8\text{O}_{20}(\text{OH})_4$) is used as the gasket material and steatite (hydrous magnesium silicate), AgCl, talc or petroleum jelly is used as the pressure transmitting medium for generating quasi-hydrostatic pressure. Bridgman anvils of cemented tungsten carbide can be used up to 10 GPa and with care

3.1 Piston -Cylinder Devices

The simplest possible piston-cylinder apparatus consists of two opposed pistons compressing the sample in a single-walled cylinder (*Figure 4*). Pistons are generally constructed of cemented tungsten carbide and the cylinder is made of high strength steel. The sample to be pressurized is immersed in a suitable pressure transmitting fluid (like silicon oil, methanol-ethanol mixture.). Hydrostatic pressure up to ~ 3 GPa can be achieved by this device. Pressure capability of this device can be enhanced further by providing external support to both the piston and the cylinder. Piston-cylinder devices are widely used for high pressure electrical resistivity, thermoelectric power, optical studies and studying compressibility of fluids.

3.2 Opposed Anvil Devices

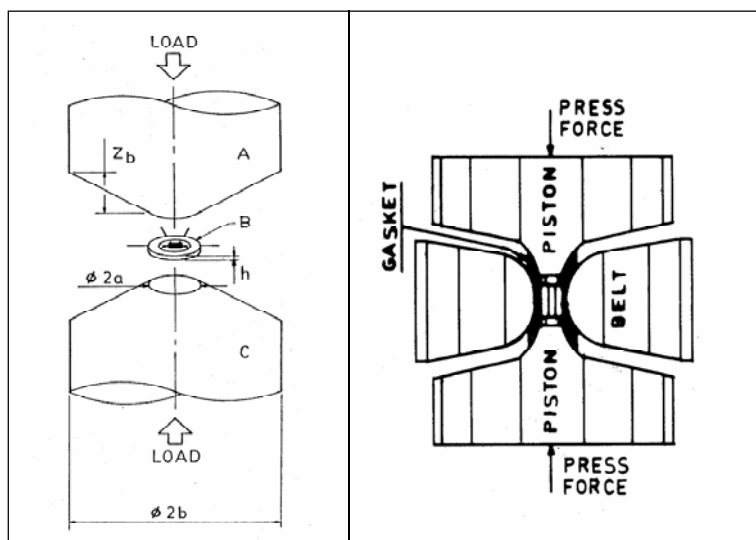


Figure 5 (left). Schematic layout of the opposed anvil device. A: upper anvil, B: gasket, C: lower anvil.

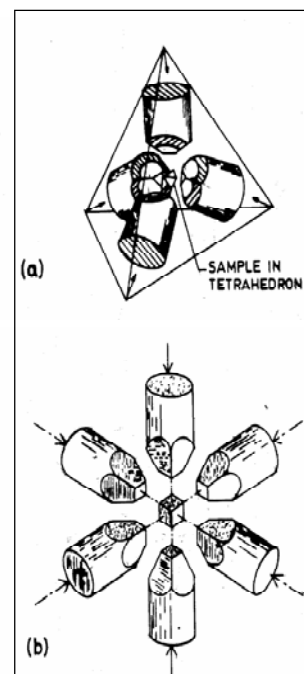
Figure 6 (right). Cross-section of a belt apparatus.

up to 18 GPa. Supported Bridgman anvils (shown in *Figure 4*) can extend the pressure up to 25 GPa.

Opposed anvil devices have smaller sample volume, but have higher pressure capability compared to piston-cylinder devices. A novel device, called the 'belt apparatus', which can be viewed as a hybrid in which the advantages of both the anvil and piston-cylinder devices are utilized is shown in *Figure 6*. Another approach to compress large volumes is through the use of multiple anvils in a symmetric tetrahedral, hexahedral, octahedral, and rhombohedral arrangement. The cubic and the double tetrahedral (two regular tetrahedrons joined together to form a six-faceted polyhedron) presses come under hexahedral devices. *Figure 7* shows the tetrahedral and cubic arrangements to generate pressures as high as 25 GPa.

These apparatus have been used for materials synthesis and for monitoring electrical resistivity, thermoelectric power, X-ray diffraction, etc. Further by incorporating suitable heating arrangement, temperatures up to 2500 K can be generated simultaneously along with pressure. The diamond anvil cell (DAC), in which the anvils are made of diamonds, also comes under the opposed anvil device and is discussed separately in the next section.

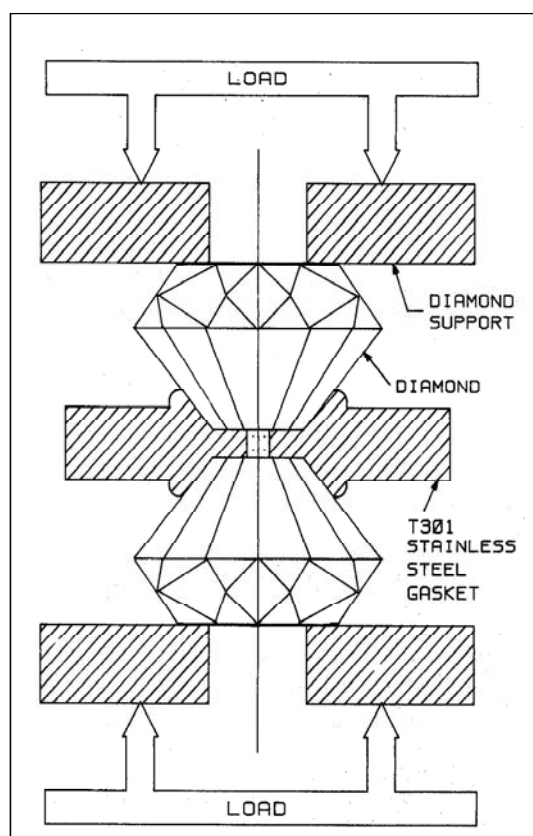
Figure 7. Geometric arrangement of tetrahedral and cubic press.



3.3 The Diamond Anvil Cell (DAC)

The pressure capability of opposed anvil devices depends on the strength of the anvil material. Since diamond has the highest strength (bulk modulus of ~ 440 GPa) among all the materials known to mankind, diamond can be used as anvils to achieve the highest pressure. Pressure as high as 560 GPa (5.6 million atmosphere) has been achieved in the laboratory using the DAC. Since diamond transmits the entire electromagnetic spectrum, it is possible to investigate matter at the highest pressures by a variety of techniques, such as X-ray diffraction, X-ray, Raman, Brillouin, IR and luminescence spectroscopy, optical reflectivity, positron and Mössbauer spectroscopy. It is possible to generate very high temperatures ~ 5000 K by focusing high power lasers (Nd-YAG or CO_2) on the pressurized sample through the transparent diamond anvils.

Figure 8. Basic principle of a diamond anvil cell.



The basic principle of a diamond anvil cell is shown in *Figure 8*. When a metal gasket is compressed between the small flat faces (culets) of two gem quality diamonds set in opposed anvil configuration, very high pressure is generated on a sample loaded in the gasket hole filled with a pressure transmitting fluid. Since the diamond anvils are very small, the sample quantity which can be compressed in the DAC is also extremely small. For example, in gasket hole of diameter $250\ \mu\text{m}$ and depth $30\ \mu\text{m}$, a sample of size $\sim 100 \times 100 \times 10\ \mu\text{m}^3$ can be loaded, which can be pressurized to ~ 50 GPa. The gasket hole and sample size should be further reduced for pressurizing to higher values.

Variations in the design of the DACs arise from different ways in which the mechanism of generating force and anvil alignment are incorporated. Five DAC designs are: NBS cell,

Bassett cell, Mao-Bell cell, Syassen-Holzapfel cell and Merrill-Bassett cell. The Mao-Bell type DAC designed and developed at IGCAR is shown in *Figure 9*.

The Mao-Bell cell consists of a piston-cylinder assembly and a pressure cell holder. The diamond anvils are mounted on a pair of semi-cylinders or combination of a half-sphere and disc (called rockers). The rockers in turn are fixed in the respective grooves of the piston and cylinder. The two diamonds meet face to face in the piston-cylinder assembly. The translation and tilting motion of the rockers are maneuvered to align the two anvils perfectly.

A metal gasket with a central hole of desired diameter is mounted between the anvils to contain the sample and the pressure transmitting fluid (liquid or inert gas). The piston-cylinder assembly is then inserted into the pressure cell holder for pressurizing the sample. Pressure is increased by simply tightening the drive screw by hand or by a spanner. The cell is now ready to be taken anywhere for carrying out the high pressure experiments.

4. Measurement of High Pressures

Pressure measurement can be classified into two categories: primary and secondary. The primary methods are based on fundamental equations relating pressure to other physical quantities. One example is the fundamental equation relating pressure (P) to the force (F) acting over area (a):

$$P = F/a. \quad (4)$$

Another example is the definition based on the Helmholtz function:

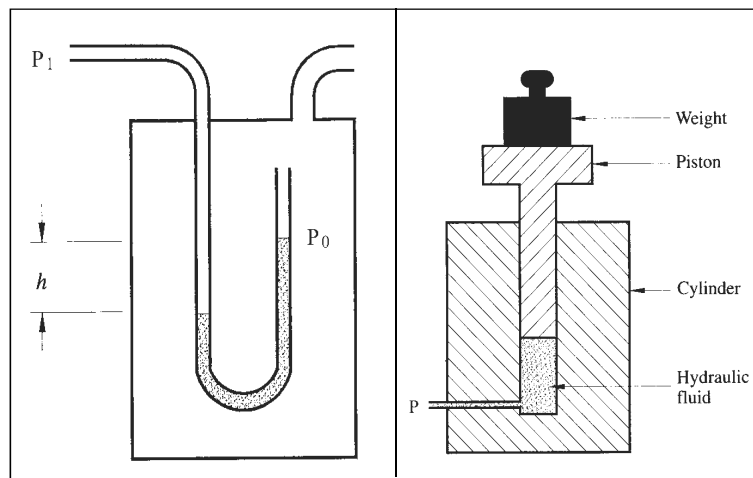
$$P = -(\delta A / \delta V)_T. \quad (5)$$

Here A is the Helmholtz function ($A = U - TS$), V is the volume, U is the internal energy, S is the entropy and T is the absolute temperature of the system. The practical realization of the second method involves models for the variation of A with T and V , so that it is no longer a primary scale.



Figure 9. Photograph of the Mao-Bell type DAC designed and fabricated at IGCAR.

Figure 10 (left). A U-tube manometer with an external gas pressure of P_0 and an internal pressure P_i .
Figure 11 (right). Schematic diagram showing the principle of a pressure balance.



Secondary methods are based on the systematic variation of any physical property of a material with pressure. The primary methods based on mercury columns and pressure balance are restricted to very small pressures (~ 1 MPa and 2.5 GPa respectively). *Figure 10* shows the schematic for a mercury column U-tube manometer and *Figure 11* the schematic of a pressure balance. In practice, pressure measurements are possible only with secondary scales. The common secondary methods for measuring high pressures are: equation of state (EOS) and fixed point method. The Ruby fluorescence method, which is employed with DAC is discussed separately.

4.1 The Equation of State Method

The equation of state of a material is a functional relationship between pressure, its volume and temperature. We are familiar with the perfect gas equation:

$$PV = nRT. \quad (6)$$

We are also familiar with van der Waals EOS:

$$P = nRT/(V-nb) - a/(nV^2) \quad (7)$$

for real gases.

In practice, pressure measurements are possible only with secondary scales.

In practice, EOS is a relationship between the volume of a material and the applied hydrostatic pressure at a specified temperature. The derivative, called the isothermal compressibility is: $K_T = -(1/V)(\delta V/\delta P)_T$. The isothermal bulk modulus B_T is just the reciprocal of K_T . Experimentally, an isotherm ($T = \text{constant}$) is measured and the equations are then fitted to the data. X-ray diffraction studies can be conveniently made on several high pressure cells, thereby affording a useful way of measuring pressure through its effect on the lattice spacing change of simple cubic solids. Volume changes at high pressures are measured and, the pressure is estimated using empirical equations of state. Some well-known empirical EOS are:

Murnaghan EOS:

$$P = (B_0/B_0') [(V/V_0)^{-B_0'} - 1]. \quad (8)$$

Birch–Murnaghan EOS:

$$P = 3/2 B_0 x^{-7} (1-x^2) [1 + c (x^{-2} - 1)], \quad (9)$$

$$c = 3/4 (B_0' - 4), x = (V/V_0)^{1/3}.$$

Vinet EOS:

$$P = 3 B_0 [(1-x)/x^2] \exp [1.5 (B_0' - 1) (1-x)], \quad (10)$$

$$x = (V/V_0)^{1/3}.$$

Here, B_0 is the bulk modulus at zero pressure, and B_0' its first pressure derivative. EOS for a number of substances such as NaCl, CsCl, KCl, Cu, Ag, Au, Pt, Mo, W, Pd, Al, Pb are being used for pressure calibration. EOS data for some well-known materials are listed in *Table 1*. Using this data and the corresponding EOS, pressure-volume relation for five materials are shown graphically in *Figure 12*. In this figure, one can clearly see the relative compression behaviour of these materials. Lead (Pb) being a soft material ($B_0 = 39.9$ GPa), is easily compressed to a reduced volume of 0.75 at 30 GPa; whereas Re, a hard material ($B_0 = 372$ GPa) can be compressed to the same reduced volume of 0.75 at a higher pressure of 195 GPa.



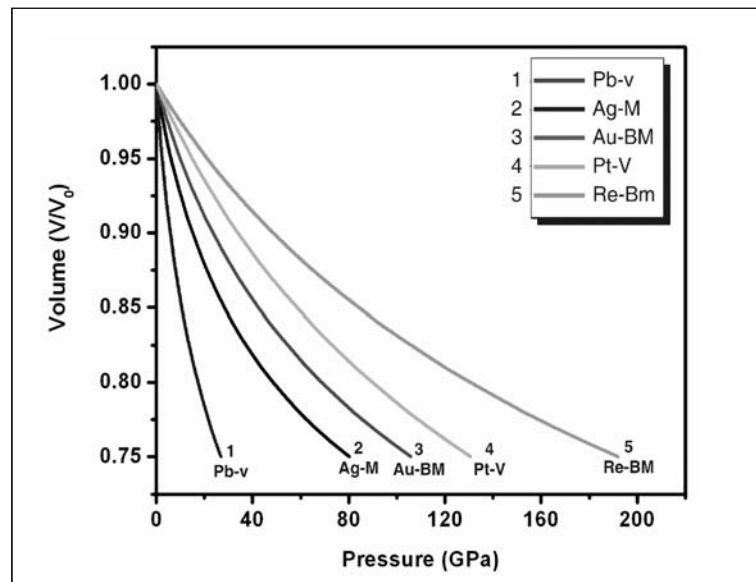
Table 1. Equation of state data of some standard materials for pressure calibration.

Calibrant	Pressure Range (GPa)	B_0 (GPa)	B_0'	EOS used
Ag	30	118	3.8	BM
Au	70	167	5.5	BM
Fe	304	157.6	5.81	BM
Pb	238	39.9	6.13	Vinet
Pt	550	262	3.96	Vinet
Re	280	372	4.05	BM
W	270	311.8	3.826	BM

4.2 Fixed Point Method

Several materials undergo phase transitions under pressure accompanied with well-marked changes in their physical properties, such as electrical resistivity, volume, specific heat. These transition points can be used as *fixed points* for pressure calibration. The acceptable fixed points for some commonly used systems are given in Table 2. Figure 13 shows the phase diagram of Bi and the resistance jumps across the phase transi-

Figure 12. Relative volume (V/V_0) vs. pressure for Ag, Au, Re, Pb and Pt computed by the EOSs listed in Table 1.



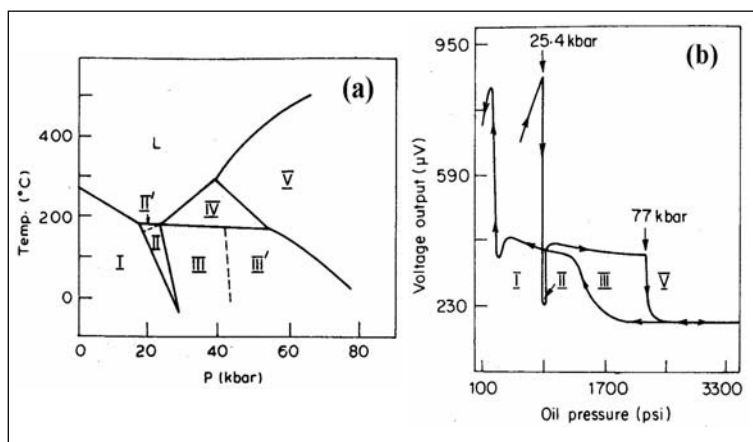


Figure 13. (a) The phase diagram of Bi and (b) the resistance jumps across the phase transitions.

tions corresponding to the fixed point pressure values of 2.55 GPa (Bi I – II), 7.7 GPa (Bi – upper) measured in the authors' laboratory. However, these fixed points are restricted to the pressure range 2 to 12 GPa only.

Apart from the above markers, high pressure can be monitored based on the changes of other physical properties such as ultrasonic sound velocities, EXAFS, resistance.

4.3 Ruby Fluorescence Method in DAC

In DAC experiments, EOS method or Ruby fluorescence is used for pressure calibration. For Ruby fluorescence calibration, a small chip ($\sim 5\text{--}10\ \mu\text{m}$) of Ruby ($\text{Al}_2\text{O}_3:\text{Cr}^{3+}$ (0.05%)) is introduced in the pressure chamber and the fluorescence is excited by a suitable laser (Ar-ion, He-Cd or He-Ne). The fluorescence is detected with an optical spectrometer. The Ruby fluorescence spectrum contains two well-defined peaks (R_1 and R_2) which shift to higher wavelengths with increasing pressure. The pressure dependence of the Ruby R_1 (692.7 nm) and R_2 (694.2 nm) shifts are used to determine pressure. Figure 14 shows a typical Ruby fluorescence spectra recorded at IGCAR. The shift of the Ruby fluorescence lines have been calibrated against standard substances to construct a pressure scale. The shifts are linear up to ~ 30 GPa at the rate of $0.365\ \text{nm} / \text{GPa}$ (or $753\ \text{m}^{-1} / \text{GPa}$ in terms of wave number). However, above 30 GPa, the scale is non-

Table 2. Fixed points for pressure calibration.

P (GPa)	Transition
2.550(6)	Bi I-II
0.68(3)	Tl II-III
5.5(1)	Ba I-II
7.7(2)	Bi III-IV
9.4(3)	Sn I-II
12.3(5)	Ba II-III
13.4(6)	Pb I-II

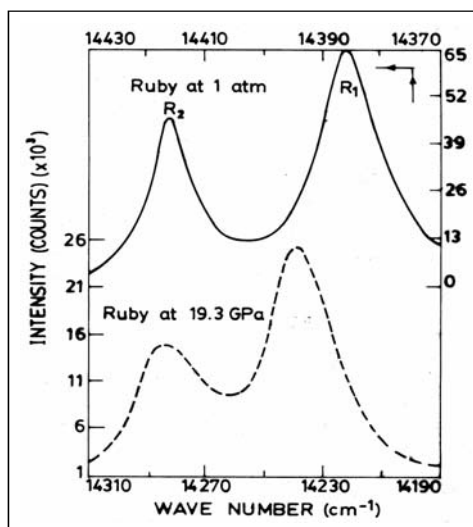


Figure 14. The Ruby fluorescence spectra at 1 atmosphere and 19.3 GPa.

Dynamic pressures or shock compressions on materials are achieved in a microsecond or less by high velocity projectile impact, laser pulses or explosives.

linear and the calibration up to 200 GPa is given by the relation:

$$P(\text{TPa}) = 0.3808 [1 + (\delta\lambda/\lambda)^5 - 1]. \quad (11)$$

Apart from Ruby, there are several other materials like $\text{Sm}^{2+}:\text{SrB}_4\text{O}_7$, $\text{Sm}^{2+}:\text{BaFCl}$, $\text{Sm}^{2+}:\text{SrFCl}$, $\text{Eu}^{3+}:\text{LaOCl}$ and $\text{Eu}^{3+}:\text{YAG}$ which are used as optical pressure sensors.

5. Dynamic High Pressures

Static high pressures on materials are achieved in seconds or longer and last for longer duration. On the other hand, dynamic pressures or shock com-

pressions on materials are achieved in a microsecond or less by high velocity projectile impact, laser pulses or explosives. Because of their fast adiabatic nature, dynamic high pressures always cause heating of the specimen. Shock pressures up to several hundred GPa and temperatures up to several thousand K are common. Such conditions are encountered during earthquakes and peaceful nuclear explosions (PNE). A shock is essentially a sharp discontinuity in stress propagating in a specimen at supersonic velocity. Fast electronic, optical and X-ray techniques have been developed to diagnose specimen response. Parameters like pressure, volume, particle/mass velocity and internal energy, i.e. P_o, V_o, U_o, E_o are used to describe the unshocked/initial state and P_s, V_s, U_s, E_s the shocked state. In an experiment, shock velocity (U_s) and particle velocity (U_p) are measured and other parameters are derived using mathematical relations governing the conservation of momentum, mass and energy across the shock wave front. A plot of the locus of any two shock parameters (such as U_s vs U_p , P_s vs U_p , P_s vs V_s etc.) is called the *Hugoniot*. From the *Hugoniot* curves, a 300 K $P-V$ isotherm can be derived by taking into account the internal shock energies.

Shock wave experiments are very important for obtaining EOS data to design nuclear weapons. The same EOSs and computer

codes are used to design and interpret a wide variety of interdisciplinary high pressure experiments. In the next part of the article, we will discuss some aspects of dynamic high pressure experiments.

Suggested Reading

- [1] P W Bridgman, *Physics of High Pressure*, Bell and Sons, London, 1958.
- [2] I L Spain, *High Pressure Technology*, edited by I L Spain and J Paauwe, Marcell Dekker, New York, Vols. I and II, 1977.
- [3] A Jayaraman, *Rev. Mod. Phys.*, Vol.55, p.65, 1983; *Rev. Sci. Instrum.*, Vol.57, p.103, 1986.
- [4] G N Peggs, *High Pressure Measurement Techniques*, Applied Science Publishers, London, 1983.
- [5] K Govinda Rajan, *Science and Technology of High Pressures*, edited by E S R Gopal, S V Subramanyan, J Ramakrishna and S Mohan, Instrument Society of India, Bangalore, Ch.2, 1984.
- [6] W F Sherman and A A Staidmuller, *Experimental Techniques in High Pressure Research*, John Wiley, Chichester, 1987.
- [7] R M hazen, *New-Alchemist, The Breaking through the Barriers of High Pressure*, Doubleday, New York, 1993.
- [8] M I Eremets, *High Pressure Experimental Methods*, Oxford University Press, London, 1996.
- [9] R J Hemley and H K Mao, *Encyclopedia of Applied Physics*, edited by G L Trigg, VCH publishers, New York, p.555, Vol.18, 1997.
- [10] W B Holzapfel and N S Issacs, *High Pressure Techniques in Physics and Chemistry: a Practical Approach*, Oxford University Press, Oxford, 1997.
- [11] R M Hazen, *The Diamond Makers*, Cambridge University Press, Cambridge, 1999.
- [12] *High Pressure Phenomena*, edited by R J Hemley, IOS Press, Amsterdam, 2002.
- [13] *J.Phys: Condens. Matter*, Vol.16, 2004, Special Issue: *Proceedings of the Joint 19th AIRAPT and 41st EHPRG International Conference on High Pressure Science Technology*, Bordeaux, 7-11 July, 2003.
- [14] *Proceedings of the Joint 20th AIRAPT - 43rd EHPRG Conference on Science and Technology of High Pressure*, edited by E Dinjus and N Dahmen, Karlsruhe, Germany, 2005.
- [15] R J Hemley, H K Mao and V V Struzhkin, *J. Synch. Rad.*, Vol.12, p.135, 2005.

Address for Correspondence
P Ch Sahu
Materials Science Division
Indira Gandhi Centre for
Atomic Research
Kalpakkam 603 102
Tamil Nadu, India.
Email: pcsahu@igcar.gov.in

